ESRF	**Experiment title:** **Study of Polyelectrolytes by ASAXS**	**Experiment number**: SC-1144
Beamline:	**Date of experiment**: long-term project from: 10/2002 to: 02/2005	**Date of report**: 14.02.2006
Shifts:	**Local contact(s)**: **Dr. T. Narayanan, Dr. M. Sztucki**	*Received at ESRF:*

Names and affiliations of applicants (* indicates experimentalists):

Dr. N. Dingenouts, Polymer-Institut, University of Karlsruhe, Germany*

Dr. S. Rosenfeldt, Physikalische Chemie I, University of Bayreuth, Germany*

Dr. A. Jusufi, Physikalische Chemie I, University of Bayreuth, Germany*

M. Patel, MSc., Physikalische Chemie I, University of Bayreuth, Germany*

Prof. Dr. M. Ballauff, Physikalische Chemie I, University of Bayreuth, Germany

Dr. F. Gröhn, MPI für Polymerforschung, Mainz, Germany

Report:

We are presently working on a long-term project, which is a continuation of our earlier experiment (SC-787, SC-1029) which is devoted to investigations of polyelectrolytes in solution using ASAXS. The central question in this field is the spatial distribution of the counterions around the macroion. The strong electric field of the macroion leads to strong correlation of the counterions with the macroion. In particular, a certain fraction of the counterions will be "condensed" to the macroion. Regarding the latter issue, ASAXS experiments can help to analyze the counterion contributions separately. This technique combines the conventional SAXS experiment with the effect of anomalous dispersion, i.e. the change of the scattering power of an element if the energy of the incidient radiation is near an absorption edge of that element. Near the absorption edge the scattering factor f of the counterions becomes a complex quantity: $f = f_0 + f' + i\,f''$ where f_0 is the energy-independent scattering factor. The factor f_0 is identical to the number of electrons in the respective ion. The quantities f' and f'' are the real and the imaginary part of the resonant part of f, and i is the imaginary unit. Fig. 1 displays the two quantities as function of energy for Rubidium ions. Hence, f' decreases considerably in the immediate vicinity of the edge which in turn leads to a decrease of the scattering factor f of Rubidium ions.

Based on the work of Stuhrmann, the ASAXS-intensity may be split into three terms:

$$I(q) = F_0^2(q) + 2f'(E)F_0(q)v(q) + [f'(E)^2 + f''(E)^2]v^2(q) \qquad (1)$$

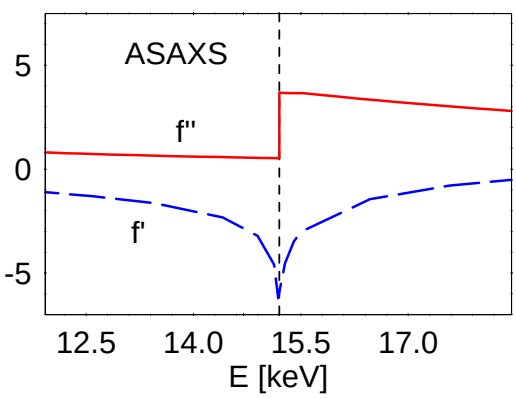

The first term is the intensity measured far below the edge as measured by conventional SAXS. The second term is the cross-term of the non-resonant amplitude and the third term which is the Fourier-transform $v(q)$ of the distribution of the counterions.

Fig.1: Dispersion of Rubidium near the K-edge: The real part f' and the imaginary part f'' are scattering factors as function of the energy.

In our experiments we had studied polyelectrolyte systems bearing Rubidium (spherical polyelectrolyte brushes, star polymers) and Strontium (brushes) counter ions.

Spherical polyelectrolyte brushes

The investigated spherical polyelectrolyte brushes (SPB, fig. 2) consist of a solid poly(styrene) core of ca. 100 nm diameter onto which long linear chains of poly(sodium styrene sulfonate) (NaPSS) or poly(acrylic acid) (PAA) are densely grafted. Using ultrafiltration the sodium counterions can be replaced by ions like Rb^+ which can be seen by synchroton radiation.

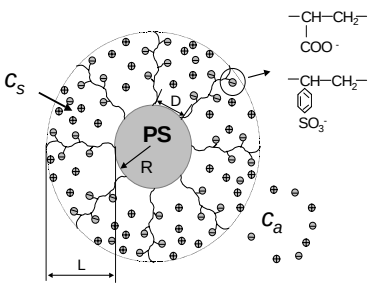

Fig. 2: Schematic representation of a spherical polyelectrolyte brush, defined by core radius R, thickness of polyelectrolyte chain layer L and concentration of ions inside (c_s) and outside (c_a) the brush.

The core of the PSB does not exhibit any resonance near the energy employed for the ASAXS studies, since it consists of elements like carbon and hydrogen. Therefore the contribution of the macro ion to the measured scattering intensity stays constant in the range of energies used in our experiments. For ASAXS the intensity *I(q)* is measured immediately below the edge and above the edge of the counter ions. The variation of *I(q)* with *f'* is then used to decompose *I(q)* according to eq. 1. The entire spherical polyelectrolyte brush can be described by two spatial distributions: i) the electron density of the macroion and ii) the spatial distribution of the counterions *v(r)* having spherical symmetry. Fig. 3 shows the scattering intensities at three different energies of the incident beam obtained for spherical polyelectrolyte brushes. From Fig. 3, it is evident that the scattering intensities are lowered as the absorption edge of the counterion ion is approached. Therefore the measured scattering intensity *I(q)* can be decomposed according to eq. 1.

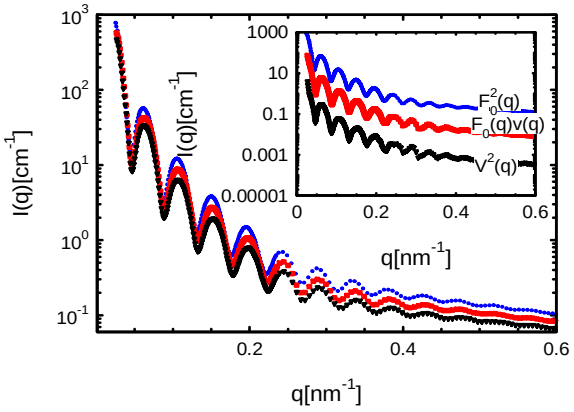

Fig. 3: Dependence of the measured scattering intensity of a PAA-brush with Rb^+ counterions on the energy of the radiation. For the sake of clarity only three data sets (difference to edge from top to bottom: -2737eV, -9 eV and -1eV) are shown out of at least 10 measured ones.

Inset: Partial scattering intensities obtained after decomposition of the measured ASAXS intensity according to eq. 1.

Our previous experiments on spherical PAA-brushes bearing univalent Rubidium counterions demonstrated that the counterions are strongly confined within the brush (*Macromolecules* **37**, 8152 (2004)). Fig. 4 shows the partial scattering intensity of the Rb^+ counterions $v^2(q)$ of a PAA brush as function of *q* and the corresponding fit assuming a radial profile of the chains with scales with r^{-2} (i.e. highly stretched chains) and an additional scattering contribution that is due to the fluctuations of the polymer chains and the counterions at the surface. From fig. 4 it can be concluded that chains of a PAA-brush are highly stretched like predicted in theory.

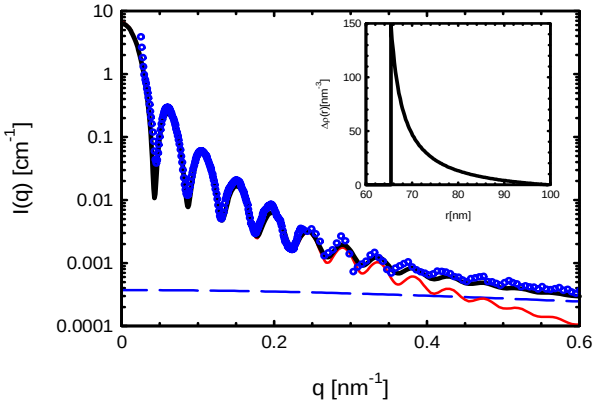

Fig. 4: Partial scattering intensity v^2 (q) as function of q with corresponding fit. The theoretical curve consists of the radial density profile displayed in the inset (solid line) and a Lorentzian term due to fluctuations (dashed line). Inset: Radial density profile of counterions.

Moreover, we studied the spherical polyelectrolyte brushes in presence of divalent counterions. In our experiments, we investigated a PSS-brush with divalent Strontium counterions (absorption of Sr^{2+} : 16104.6 eV). In these studies we are able to determine all the three partial intensities for that quenched brush system (fig. 5). The decrease of the different intensities and the positions of the maxima are identical, i.e. the ratio of $F_0(q)\nu(q)$ to $\nu^2(q)$ is constant. From the analysis of the data obtained for divalent counterions, it is clear that the Strontium ions too, as compared with the Rubidium ions decorate the polyelectrolyte chains and are strongly confined within the brushes

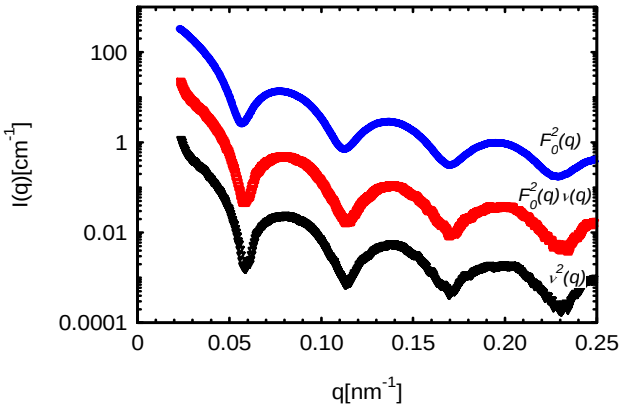

Fig.5: Result of the decomposition of the measured ASAXS intensity of a PSS-Brush with Sr^{2+} ions according to eq. 1.

Star branched Polyelctrolytes

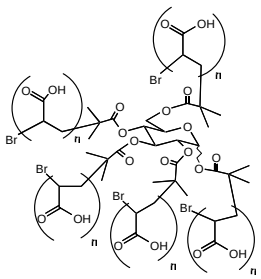

Fig. 6: Chemical structure of star shaped polyelectrolytes.

We present our preliminary results on star branched polyelectrolytes. Here we have used star branched polyelectrolytes as shown in Fig 6, which consists of arms of poly(acrylic acid) (PAA), with varying number of arms and degree of polymerization. The polyelectrolyte is formed by titration of polyacid with RbOH solution. A series of SAXS and ASAXS experiments were carried out at different concentrations c, degrees of polymerization P_n and degrees of dissociation α.

Fig 7 shows the SAXS results obtained for star-shaped polyelectrolytes comprising of 21-arms, P_n=60 and α=0.7. It is evident from Fig. 7, that an ordering phenomenon in the vicinity of the overlap volume fraction ϕ^* is observed, which vanishes on either side of the overlap volume fraction (calculated ϕ^*~0.44 vol.%). The shift of q_{max} towards higher q-values as a function of increased concentration, is due to the decrease in the interparticle distance between the polyelectrolyte chains. On the other hand, as the concentration increases the peak disappears gradually. After literature (Heinrich et al., Eur. Phys. J. E. 4, 131 (2001)) this phenomenon can be attributed to the interpenetration of star polyelectrolytes.

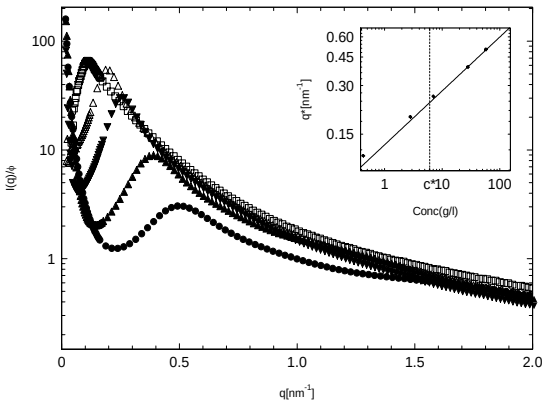

Fig. 7: Measured scattering intensities of a PAA star at different concentrations (0.4g/l, 1.3g/l, 2.8g/l, 7.1 g/l, 28.2g/l and 58.0g/l(left to right)). Inset: Variation of q as function of concentration.*

As in the case of spherical polyelectrolyte brushes, we carried out the analysis of the ASAXS data for star-shaped polyelectrolytes in the similar fashion. All the three terms relating to eq. 1 can be extracted from this data as well. Fig 8. shows the three partial intensities as a function of q for a PAA-star solution having mean values of 21 arms, P_n=60 and α=0.7. Additionally the results of a MD simulation of a star polymer are given. As expected from these simulations, the Rb^+ counterions are closely correlated to the polyelectrolyte chains for star shaped polyelectrolytes in that case, too. The deviation between the results of the ASAXS experiment and the simulation may be due to the influence of concentration and polydispersity.

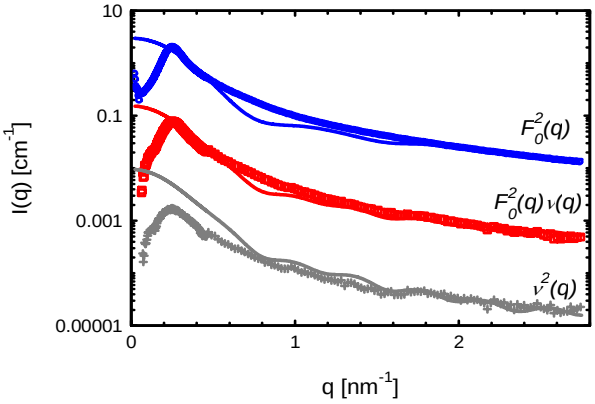

Fig. 8: Partial scattering intensities of a PAA star with f=21, P_n=60, α=0.7 and a concentration in the immediate vicinity of ϕ^* (symbols). The lines denote the corresponding intensities predicted by a MD simulation done by A. Jusufi in our group.

At present, we study the influence of different arm functionalities f on the correlation of the counterions to the polyelectrolyte chains. In fig. 9 the partial scattering intensities $F_0(q)$ and $v^2(q)$ are shown for two stars differing in the number of arms. At low q-values the difference between the two systems can be explained mainly by the different size and different concentration of the corresponding stars. For q>0.6 nm^{-1} the decrease of the scattering intensities $F_0(q)$ is similar. A possible explanation would be that the scattering is dominated by the scattering of the polyelectrolyte chains in these regime. MD simulations done in our group have shown that the counterions can possess three different states: they can be condensed along the chains, inhomogeneously distributed inside the star or they can be outside of the star. The results of the simulations leads to the conclusion that the counterions in the case of low star numbers are not strictly confined in the star. With increasing number of arms the counterions and the polyelectrolyte chains are come closer to each other. At high enough arm numbers the counterions are fully confined within the polyelectrolyte star.

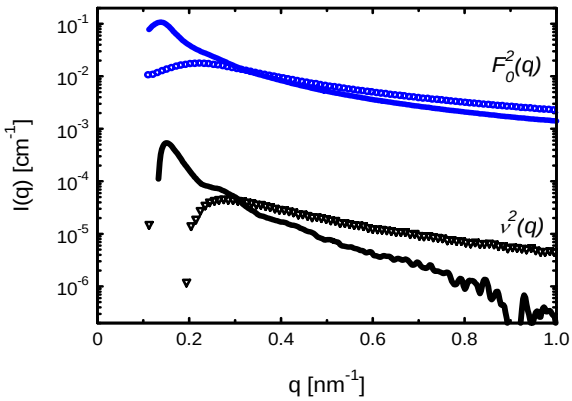

Fig. 9: Partial scattering intensities $F_0(q)$ and $v^2(q)$ after decomposition of the ASAxS intensity of PAA stars. The different stars had the following parameters: f=8, P_n=101, α=0.7, c=2.6g/l (symbols) and f=21, P_n=97, α=0.7, c=1.9g/l (lines).

The different states of counterions can be tuned by additional salt. Fig. 10 shows the influence of adding 0.02mol/l RbCl to a 21-armed stars bearing already Rubidium counterions. As expected, the decrease of the slopes is most pronounced for $v^2(q)$ due to a appreciable amount of counterions outside the star. A detailed analysis of these results as compared with computer simulations is currently under investigation.

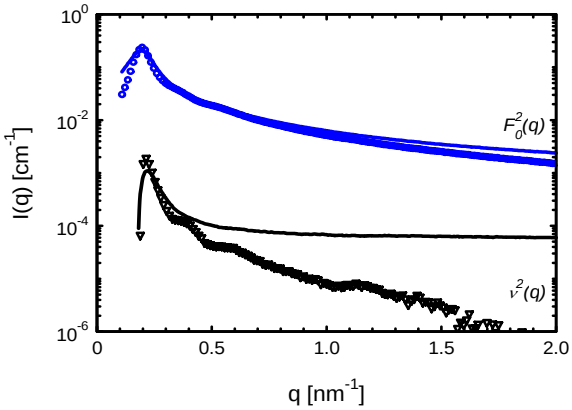

Fig. 10: Partial scattering intensities $F_0(q)$ and $v^2(q)$ after decomposition of the ASAXS intensity of a PAA-star solution without (symbols) and with additional (0.02 mol/l RbCl, lines) salt . We used a star with f=21, P_n=97, α=0.7 and c=6.6g/l.